

A low speed single barrel pellet injector and its application to complementary study on ablatant in LHD

J. S. Mishra¹⁾, R. Sakamoto²⁾, G. Motojima²⁾, H. Yamada²⁾

¹⁾ Graduate University for Advanced Studies, SOKENDAI, Toki 509-5292, Japan

²⁾ National Institute for Fusion Science, Toki 509-5292, Japan

(Received: 20 November 2009 / Accepted: 29 March 2010)

A simplified calculation considering the three dimensional helical magnetic field and $\mathbf{B} \times \nabla \mathbf{B}$ drift was carried out to study the effect of injection location on plasmoid drift. From the calculations different injection possibilities are considered around the torus for the experiment.

A low speed single barrel pellet injector has been designed for alternative injection in LHD. A pellet is being injected by the combined operation of mechanical punch and pneumatic propellant system. The shape of the pellet is cylindrical of $3 \text{ mm}\varphi \times 3 \text{ mm}l$. Pellet injection speed ranges between $100 \sim 600 \text{ m/s}$ but maximum injection speed during operation is constrained to survivability through the curved guide tube. Different curved guide tubes are designed for efficient launching of pellet to particular locations of LHD.

Keywords: LHD, Pellet Injector, Solenoid Punch, Plasmoid, $\mathbf{E} \times \mathbf{B}$ drift, Guide tube

1. Introduction

Pellet injection using isotopes of Hydrogen has been proved to be a promising method for magnetically confined plasma devices such as tokamak and stellarators/helical devices [1–3]. Improved plasma properties obtained for a pellet injected NBI plasma in Heliotron E, however for a highly peaking density profile plasma becomes unstable [4]. But in Large Helical Device (LHD) a high density (up-to 10^{21}), stable with low diffusion operational regime, so called Internal Diffusion Barrier (IDB) has been discovered using pellet injection [5]. It has been experimentally observed that fueling efficiency is more for high field side injection compare to the low field side injection of the torus [6]. This is due to the drift of the ablatant towards the Low field side(LFS) of the torus [7, 8]. This drift reported is supposed to be due to the $\mathbf{E} \times \mathbf{B}$ force on the ablating ionized cloud by its self-consistent electric field, produced by the $\mathbf{B} \times \nabla \mathbf{B}$ drift of ions and electrons inside it [9]. Technological difficulty restricts higher pellet injection speed for core fueling. It can be seen from equation (1) that, there is a poor dependence of normalized penetration depth λ/a [10] on injection speed in comparison to plasma temperature. Therefore it will be a major issue to inject a pellet into plasma core from LFS for the next generation high temperature and large volume plasma devices like ITER. Therefore considering the above discussed kind of drift, it is viable to inject a pellet from HFS of the device for better fueling efficiency and it is also planned for ITER.

$$\frac{\lambda}{a} = CT_e^{-5/9} n_e^{-1/9} r_p^{5/9} v_p^{1/3} \quad (1)$$

Where T_e, n_e, r_p, v_p are the plasma temperature and density, pellet radius and speed respectively.

LHD has major radius, averaged minor radius, magnetic field and plasma volume 3.9 m, 0.6 m, 2.9 T and 29 m^3 respectively. LHD has a set of $1/m=2/10$ continuous superconducting helical coils which generates the magnetic confinement field. Since the helical modulation is superimposed to the toroidicity, additional High Field Side (HFS) appears under the helical coil and varies from one location to other, hence the HFS side is not always inboard to the vacuum vessel as in the case of tokamak. Therefore, one cannot simplify the magnetic field strength distribution like $\mathbf{B} \propto 1/R$ as in axis symmetric tokamak field. A complementary study, focusing on differences of the magnetic field configuration between the helical device and tokamak, is one of the approaches to understand the effect of pellet plasmoid drift on the fueling efficiency in LHD. Previous study on LHD considering $\nabla \mathbf{B}$ drift for the coil side injection (CSI) is still premature due to the lack of local density measurements [11]. The objective of present study is to know the effect of magnetic configuration on pellet injection locations by considering the $\nabla \mathbf{B}$ induced drift and subsequent density redistribution process for different pellet injection locations in LHD.

LHD is equipped with a multi barrel high speed($\approx 1200 \text{ m/s}$) pneumatic pipe gun type pellet injector [12]. Bended guide tubes are needed for injection locations other than outboard side of the torus. Deterioration of pellet mass inside it limits the application of high speed pellet injector [13], hence a low speed pellet injector has been designed. In following sections finding of a suitable location for pellet injection considering the $\nabla \mathbf{B}$ effect and development of a low

author's e-mail: mishra@lhd.nifs.ac.jp

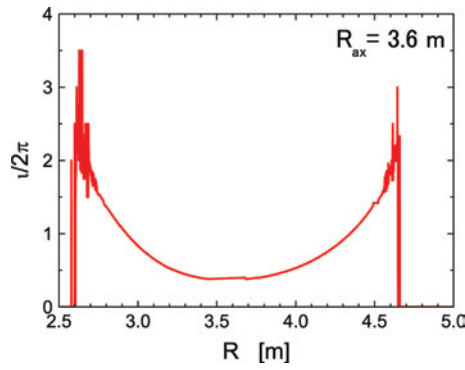


Fig. 1 Rotational transform along the major radius direction for $R_{ax} = 3.6$ m.

speed injector is being presented.

2. ∇B and plasmoid drift calculation

A pellet injected into the plasma heated mainly by electron heat flux from the plasma. After the pellet ablation cloud is established, ablated material is ionized and forms a high-density and low temperature plasmoid. A polarization field arises due to the drift of ions and electrons in inhomogeneous magnetic field. This electric field interacting with the magnetic field pushes the ablating materials down the magnetic field gradient and hence affects the fueling efficiency. Many processes like Alfvén wave generation and overlapping of flux tubes after the plasmoid expands half a toroidal turn along the field lines tend to compensate the polarization field and hence the drift of the plasmoid [9]. Thus it is important to study the ∇B drift on plasmoid for a non-axis symmetric magnetic field device like LHD.

LHD has helical ripples and rotational transform due to external helical coils. Fig.1 indicates the variation of rotational transform along the major radius in the case with magnetic axis position $R_{ax} = 3.6$ m. The rate of change of magnetic field on edge region along the toroidal direction is very high and this is less for inner region of plasma. From the field line tracing along the toroid, direction of ∇B and poloidal position for a point on the field line that begins from the pellet ablation location was identified. Fig.2(a) indicates the field line calculation at $\rho = 0.9$ for a plasmoid starting from the ablation point along the direction of pellet injection from the LFS outboard (On mid-plane) of the Torus. For $\rho = 0.9$ ∇B makes 9 revolutions poloidally for one toroidal turn and also the poloidal position variation rate is high. Therefore an electric field which drives the density redistribution may not be formed sufficiently inside the plasmoid. Vector plot shown in Fig.2(b) also indicates that the magnitude and direction of ∇B is not constant along the magnetic field line (Blue arrows for the case of

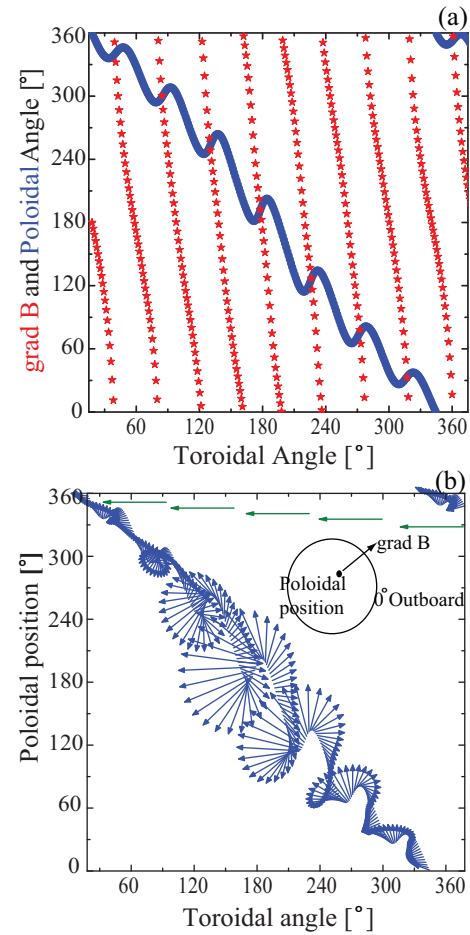


Fig. 2 (a) Variation of ∇B direction (red star) and poloidal position (Angle) of field line (continuous line) (b) Vector plot of ∇B (Blue arrows) along toroidal line projected on to poloidal plane (for LHD). Green arrow shows the ∇B direction in the case of tokamak

LHD). A comparison for the case of a same aspect ratio tokamak for the same ρ value represented by the green arrows indicates that ∇B is always towards inboard side of torus and there is a little variation of this.

To know the effect of $E \times B$ drift on pellet injection location a simple calculation based on the effect of $B \times \nabla B$ drift on plasmoid was performed for a number of pellet injection locations of the torus. A discrete set of points on the direction of pellet injection is presumed. A plasmoid is assumed to be at these sets of points as soon as the pellet ablation completes. Expansion of the plasmoid from that point along the toroidal magnetic field direction was taken into consideration. The geometry of LHD indicating HFS, LFS, horizontally elongated, vertically elongated section and ∇B direction is shown in Fig.3. A comparison between the case for a HFS and a LFS injection is shown in Fig.4. The LFS location is horizontally elongated outboard side and the HFS side (Coil side)

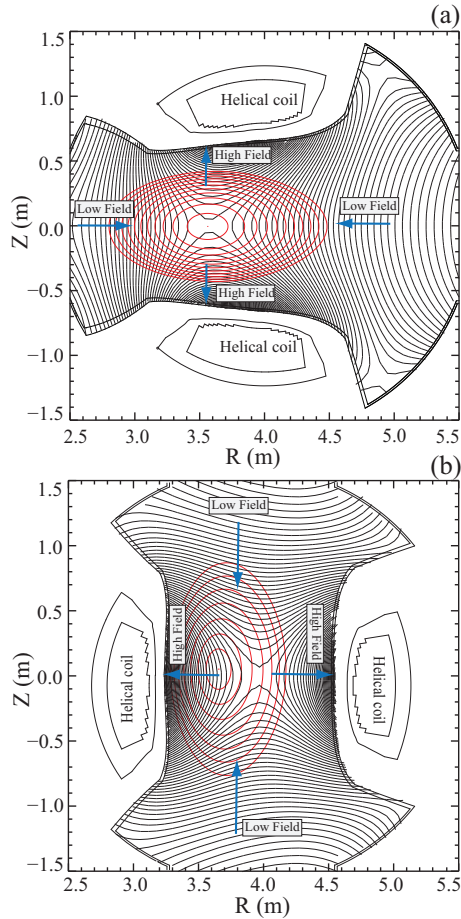


Fig. 3 Contour plot (Black line) of magnetic field strength at a (a) Horizontally elongated cross section and (b) vertically elongated cross section of LHD. Blue arrows indicates the direction of ∇B and colored ellipses are the magnetic flux surfaces. Location of HFS positions are near the helical coils.

is taken at the vertically elongated inboard side of the torus. The vector plots shown are the projection of drift direction along the field line on the poloidal plane of the LHD. The black arrow indicates the pellet ablation and plasmoid formation region along the pellet trajectory. Colored lines indicate the 60 cm expansion of plasmoid along the field line up to which plasmoid expansion can be observed. For the LFS, drift is less and nearly constant along the field lines compare to HFS and the drift direction is always out of the torus. For the HFS drift is significantly high and in-fact for this position drift is maximum compare to all other locations. Due to space constraint injection of a pellet from the inboard coil side is not possible, hence a different approach by injecting a pellet from a low field side pointing to a location close to helical coil is being considered(Fig.5). Fig.6(a) shows the drift direction for an inner port injection pointing to a region close to helical coil above the mid-plane at $z=0.13\text{m}$ (51° I port cross section). A similar approach also

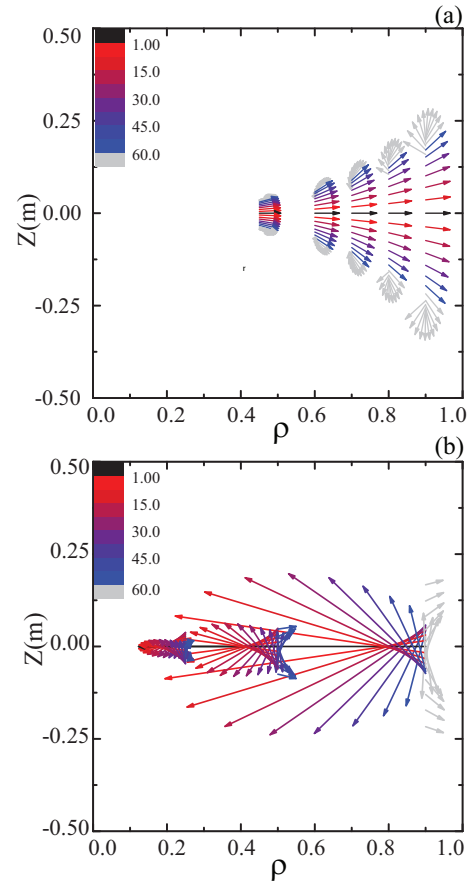


Fig. 4 $E \times B$ drift direction along the field line projected on to poloidal plane for (a) LFS outboard consideration and (b) HFS inboard consideration. Colored lines indicates the plasmoid expansion length along the field line direction.

considered(Fig.6(b)) for upper port injection from a vertically elongated section. For both the cases calculation suggests a significant amount of drift effect along the field line towards the center of the torus. Based on the calculations following injection possibilities are considered for the experiments, (1) Horizontally elongated outer port injection (2) shallow angle inner port injection and (3) Shallow angle upper port injection. First one is the LFS while other two possibilities considered as the HFS injection.

3. Pellet Injector

A single barrel in-situ pipe gun type pellet injector has been developed for alternative injection in LHD. Due to inadequate floor space the overall dimension of the pellet injector is kept minimized. A solenoid operated mechanical punch is used to initialize the pellet motion. It also helps to minimize the total length of the injector by minimizing the requirement for differential pumping system by reducing He propellant gas. A schematic of the injector is shown in Fig.7. In following subsections a detail of various parts of the

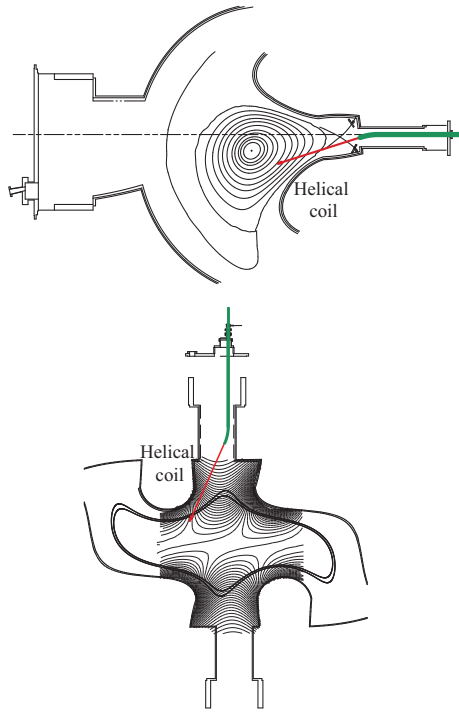


Fig. 5 Upper figure: Shallow angle inner port injection at $z=0.13\text{m}$ (51° cross-sectional view) close to helical coil; Lower figure: Shallow angle top port injection to a HFS (outboard side view). Guide tube with bending at the end towards the HFS and pellet path are shown by green line and red arrow respectively.

pellet injector is presented.

3.1 Cryogenic Chamber

For the pellet formation a Gifford-McMahon cycle compact cryo-cooler is being used. The GM-cycle cryo-cooler has the advantage that it is free from replenishment of cooling media such as liquid helium and can be easily and remotely operate by using the common utilities such as cooling water and electricity inside experimental hall. The cooling capacity of this cryocoller is 10 W at 8 K on the second stage. The first stage at 40 K temperature is connected to a cylindrical thermal shield ($18\text{ cm}\varphi \times 35\text{ cm}\ell$) made up of copper. The second stage is connected to the heat sink made up of Copper. A barrel of internal diameter 3 mm made up of stainless steel is brazed to a Cu disk of 3 mm width, which is connected to the heat sink. All these equipments are placed inside a vacuum chamber which maintains a vacuum level of the order 10^{-5} Pa. A turbomolecular pump of capacity $0.06\text{ m}^3/\text{s}$ is connected to this chamber. It takes around 1.25 hour to cool down the heat sink from the room temperature to 4 K. A heater is being installed to maintain the temperature at required level. The injector will be ready for operation after one and half hour of switching on cooling down. As the heat load

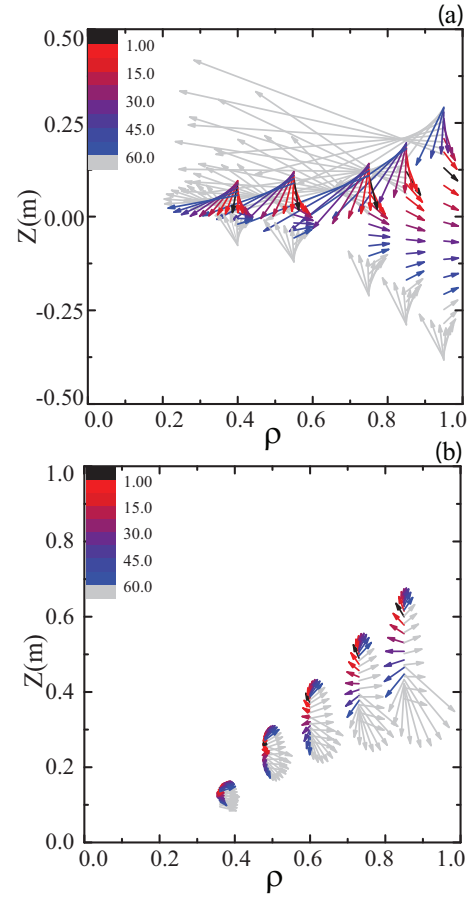


Fig. 6 $E \times B$ drift direction along the field line projected on to poloidal plane for for (a) inboard side shallow angle consideration and (b) upper port shallow angle consideration. Colored lines indicates the plasmod expansion length along the toroidal direction.

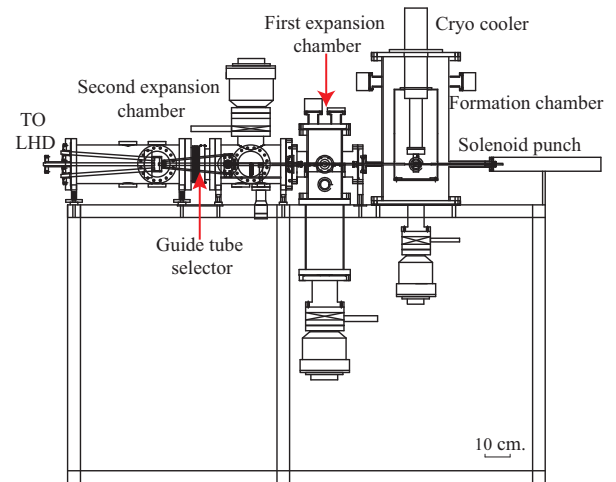


Fig. 7 Schematic of Punch mechanism pellet injector

to heat sink is negligible and rate of cooling is very high, temperature increase due to a pellet injection can be recovered quickly and it can be ready for the next pellet within few seconds.

3.2 Pellet Size and Speed

In LHD cylindrical pellet size of $3 \text{ mm}\varphi \times 3 \text{ mm}l$ is regularly injected to the NBI heated plasma by multi barrel pipe gun injector. Hence the same size pellet will be used for the above-discussed kind of pellet injection. A pellet contains 10^{21} hydrogen atoms, hence for a plasma of volume 30 m^3 increase of density 3×10^{19} is expected. As the pellet will be launched through the curved guide tubes, pellet launching speed will be depend on the survivability of the pellet through it, which is $\approx 300 \text{ m/s}$ but the injector can be operated at higher speed.

3.3 Pellet Launching

A pellet needs high pressure or a little warm up to break away from the freezing zone. For the case of high pressure, the pellet is being accelerated to higher speed. The pellets with higher speed cannot be survive through the curved guide tube, and again due to space constraint the injector dimension is minimized. Therefore to balance these situations a solenoid punch is added to the breech side of the injector which initializes the motion of the pellet from the freezing zone. After that a small burst of He propellant gas can be add to accelerate it to higher speed. The propellant gas can be easily removed by the two stage differential pumping system. Using this technique the velocity of pellet can be controlled precisely and with addition of more gas the pellet can be reach up-to high speed. The punch head, operated by a solenoid used in this system is originally procured from the Oak Ridge National Laboratory (ORNL)

3.4 Vacuum system and guide tube

Two stage differential pumping system has been installed to restrict the inflow of propellant gas into the plasma chamber. The volume of 1st and 2nd expansion chamber are 0.015 and 0.02 m^3 respectively. Both the expansion chambers are connected to turbo-drag pumps of pumping speed $0.25 \text{ m}^3/\text{s}$ and $0.5 \text{ m}^3/\text{s}$ respectively. Expansion chambers-1 and 2 are maintained a vacuum level of 10^{-5} and 10^{-6} Pa respectively. Considering maximum of 1 Pam^3 propellant gas required for single pellet injection, the characteristic curve for differential pumping system can be calculated from the following equations.

$$V_1 \frac{dP_1}{dt} = I_{acc} + C_{12}(P_2 - P_1) - S_1P_1 + L_1 \quad (2)$$

$$V_2 \frac{dP_2}{dt} = C_{12}(P_1 - P_2) - S_2P_2 + L_2 \quad (3)$$

Where I_{acc} , P_i , V_i , S_i , C_i and L_i denote propellant gas inflow rate, pressure of the stage i, volume of the stage i, pumping capacity of the stage i, conductance between the stages i and i + 1 which are connected by guide tube and leak and/or degassing

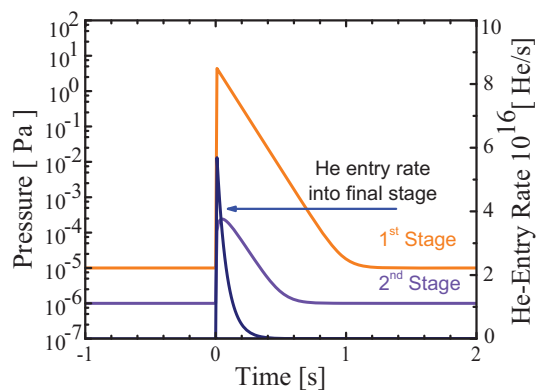


Fig. 8 Vacuum characteristic curve (Theoretically calculated value; experimental data is not available) for two stage differential pumping.

rate of the stage i, respectively. Fig.8 shows the characteristic curve for the differential pumping system based on the above calculations. The vacuum level of the first expansion chamber(1st stage) increases to 5 Pa just after the pellet injection as there is a direct inflow of propellant gas into this chamber, but due to differential pumping the vacuum level of 2nd stage increases approximately to 10^{-4} Pa and the increase in pressure in this chamber can be recovered within short interval of time.

The final expansion chamber is equipped with a guide tube selector and three guide tubes to launch a pellet from different locations. The guide tube selector can be controlled remotely during experiment . A schematic of the pellet injector with guide tubes used for the different pellet injection locations are shown in Fig.9. The total length of the guide tube for low field side is 2.2 m with two bending. The inner port guide tube is 20 m length and the upper port guide tube is of 14 m length with five bending in each.

Pellet erosion occurs by the centrifugal force, due to the curvature of the guiding tube. The tensile strength σ_t of a pellet in terms of centrifugal force is given by [14]

$$\sigma_t = \frac{mv_p^2}{AR} \quad (4)$$

Where m is mass of the pellet, v_p is velocity of Pellet, A is area of the pellet in contact with guide tube wall and R is bending radius of the guide tube. Taking $\sigma_t = 0.1 \text{ MPa}$ [15] at 10 K temperature for a Hydrogen pellet and A = 10 % of total surface area, the relation between v_p and R can be written as $v_p = 400\sqrt{R} \text{ m/s}$. For $R = 0.8 \text{ m}$ a pellet up to a speed of 350 m/s can be delivered intact. An intact ratio of 65% and 100% at $v_p \leq 350 \text{ m/s}$ and 300 m/s respectively has been obtained using the guide tube of $R = 0.8 \text{ m}$ [13]. Hence all the guide tubes used are of bending radius 0.8 m .

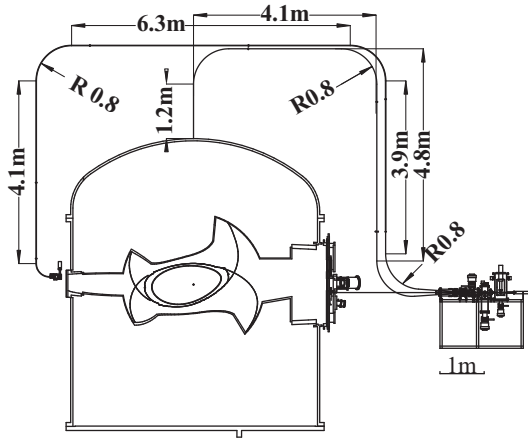


Fig. 9 Schematic of guide tubes connected between pellet injector and inboard, outboard, upper port of LHD.

3.5 Injector diagnostics

The injector is equipped with two light gate system to measure the pellet speed by the time of flight measurement between two fixed positions. Each light gate consists of a laser and photodiode. A shadow-graph system consists of a CCD camera and a flash lamp of 180 ns pulse width is installed on the 2nd chamber to image the pellet during its passage in the field of view of the camera. From the size and density, pellet mass can be measured, which will be useful for fuelling efficiency calculations. Fast photodiodes and imaging fiber will be used for the pellet ablation studies inside the plasma.

3.6 Controls and Data acquisition

Due to inaccessibility of the experimental hall, the pellet injector should be controlled remotely during plasma operation. A PC based control system is developed using National Instruments Compact Field Point (CFP) controller, input output card and LABVIEW software. CFP placed near the injector in experimental hall can easily be accessed via ethernet network from LHD control room. All the vacuum valves and pumps are controlled by CFP. Also the pellet formation cycle synchronized with 160 second before plasma discharge is controlled by CFP, whereas timing signal for the solenoid punch and fast valves are controlled by software developed on visual basic platform. The pressure and temperature data of the injector is also collected by CFP analog modules. Diagnostic system data's such as light gate shadowgraph and fast photodiode data is collected by fast ADC.

4. Summary

A simple calculation considering the ∇B drift on plasmoid in non axis symmetric magnetic field of LHD was performed for different pellet injection possibilities. Calculation shows significant drift for shallow

pellet injection compare to LFS injection when the pellet plasmoid approaches a region close to helical coil. Based on the calculation three different injection locations are considered for experiment. Curved guide tubes of bending radius 0.8 m are installed for pellet launching. Pellet mass erosion occurs at high speed while passing through bended guide tubes. Hence a pellet injector of low injection speed using mechanical punch and small amount of propellant gas was designed. Pellet injection and comparison of $E \times B$ drift effect with the theoretical models will be carried out to investigate the ablation and mass deposition process for optimization of the pellet injection location.

Acknowledgements

The support of technical peoples involved in making of this injector is greatly acknowledged. This work is supported by the Ministry of Education, Sports, Culture, Science and Technology, Grant-in-Aid for Scientific Research (S) 20226018.

References

- [1] S.L. Milora, Nucl. Fusion 35, 657 (1995).
- [2] B. Pegourie, Plasma Phys. Control. Fusion 49, R87 (2007).
- [3] R. Sakamoto, Nucl. Fusion 4, 38, (2001)
- [4] S.Sudo et al, Fusion technology, Vol. 1, 656-660 (1992)
- [5] R. Sakamoto, Nucl. Fusion 49, 085002, (2009)
- [6] P.T.Lang Phys. Rev.Lett., 79, 1487(1997)
- [7] H. W. Muller, Phys. Rev. Lett. 83, 2199 (1999)
- [8] J D Kloe, Phys. Rev.Lett, 82, 2685 (1999)
- [9] Rozhansky V, Plasma Phys. Control. Fusion 46, 575 (2004)
- [10] L.R.Baylor, Nuclear Fusion 37, 4 (1997)
- [11] R. Sakamoto, Nucl. Fusion 44, 624 (2004)
- [12] H. Yamada et al., Fusion Eng. Des. 49-50, 915(2000).
- [13] S.K. Combs et al, Fusion Eng. Des. 58-59, 343(2001).
- [14] S.Sudo et al, Fusion technology, 14, 1334(1988).
- [15] S.K. Combs, Rev. Sci. Instrum. 64, 1679 (1993).